Ionics (2017) 23:2143–2152
DOI 10.1007/s11581-017-2057-2

ORIGINAL PAPER

SGO/SPEN-based highly selective polymer electrolyte membranes for direct methanol fuel cells

Tao Cheng[1] · **Mengna Feng**[1] · **Yumin Huang**[1] · **Xiaobo Liu**[1]

Received: 30 October 2016 / Revised: 2 March 2017 / Accepted: 2 March 2017 / Published online: 18 March 2017

Abstract In this study, proton-exchange membranes (PEMs) consisting of sulfonated poly(arylene ether nitrile) (SPEN) have been successfully prepared by incorporating a different amount of sulfonated graphene oxide (SGO). Incorporation of SGO can improve proton conductivity and reduce the methanol permeability. Besides, the existence of the intermolecular interactions between SPEN and SGO can improve the interfacial compatibility between filler and matrix. The resulting composite membranes show better mechanical property, proton conductivity and lower methanol permeability compared to that of pure SPEN. Furthermore, the composite membrane with 1 wt% SGO possesses good interfacial compatibility, exhibiting excellent proton conductivity (0.109 S/cm at 20 °C and 0.265 S/cm at 80 °C) and low methanol permeability (0.17×10^{-6} $cm^2 \cdot s^{-1}$ at 20 °C). So it achieves the highest selectivity (6.412×10^5 $S \cdot s \cdot cm^{-3}$), which is about 14 times higher than that of Nafion 117. All these data indicate that the SPEN/SGO composite membranes have good potential for applications in direct methanol fuel cells.

Keywords Sulfonated poly(arylene ether nitrile) · Sulfonated graphene oxide · Highly selective · Composite membrane · Proton exchange membrane

✉ Yumin Huang
hym@uestc.edu.cn

✉ Xiaobo Liu
liuxb@uestc.edu.cn

[1] Research Branch of Advanced Functional Materials, School of Microelectronic and Solid-State Electronic, High Temperature Resistant Polymers and Composites Key Laboratory of Sichuan Province, University of Electronic Science and Technology of China, Chengdu 610054, China

Introduction

In recent years, with the development of science and technology, direct methanol fuel cell (DMFC) has received tremendous attention because of its high power density, high efficiency and pollution free [1–3]. According to the difference between the supply of fuel solution, DMFC is divided into two types: active and passive DMFC. Compared to active DMFC, the passive DMFC is compact, simple in construction and has low parasitic power losses. Thus, passive DMFC is a good choice for conventional battery replacement for portable application [4, 5]. The passive DMFC performance is related to the following factors: the size and shape of active area, proton exchange membrane, cell orientations, environmental conditions, the optimum methanol concentration, catalyst loading on the anode and cathode side, designs of current collectors (CC) and so on [6–11].

Proton exchange membrane as a key component of DMFC, can transfer proton from anode to cathode and prevent the mixing of reactants [12, 13]. At present, the commercial proton exchange membrane used in DMFC, is Nafion because of its high conductivity and excellent chemical stability. But the high cost and high methanol crossover restrict its extensive uses [14–16]. Therefore, it is urgent to modify Nafion to solve existing problems or develop a novel material for fuel cell application.

To address these problems, many sulfonated aromatic polymers have been extensively investigated as proton exchange membranes. Sulfonated poly(arylene ether nitriles) (SPEN) have attracted our attention owing to its excellent comprehensive properties such as outstanding mechanical properties, high chemical and thermal stability [17–21]. Besides, the polar nitrile groups in SPEN can restrain the membrane swelling and enhance the adhesion property with electrode layers for long-term fuel cell operation [22]. However, with the increase

of sulfonation degree, the dimensional stability of membranes reduces obviously, resulting in a decrease in mechanical properties. As is known, the properties of the membranes can be improved by blending with filler. Therefore, organic-inorganic hybrid is a promising approach to solve these problems [23, 24].

Recently, graphene oxide (GO) has been investigated intensively because of its excellent electrical properties, unique two-dimensional structure and large specific surface [25–28]. GO which contains hydrophilic oxygen-containing functional groups (e.g. epoxy and hydroxyl) can be further modified by introduction of various functional groups to expand its application. For example, sulfonated graphene oxide (SGO) as an excellent filler has been applied to composite proton exchange membranes [29–33]. The composite membranes show low methanol permeation and high proton conductivity. To our best knowledge, typical methods for preparing SGO is the use of an aryl diazonium salt or chlorosulfonic acid. Although significant methods have been made in this area, developing a new and simple method for the synthesis of SGO is still in high demand. In addition, cyano groups in SPEN can increase the intermolecular interactions between polymer chains and SGO, making the composite membranes more compact, which is favour for the reduction of methanol permeability.

Herein, in this work, SGO was obtained by using a simple, convenient and cheap way. The sulfonic acid groups were introduced into GO via direct sulfonated method and the SGO/SPEN composite membrane was prepared by solution-casting method. Meanwhile, its mechanical properties, thermal properties, proton conductivity and methanol permeation were also investigated in detail.

Experimental

Materials

2,6-Difluorobenzonitrile (DFBN), 4,4′-biphenol (BP) and potassium 2,5-dihydroxybenzenesulfonate (SHQ) were purchased from Sigma-Aldrich. Sulphuric acid (H_2SO_4, AR), phosphoric acid (H_3PO_4, AR) and potassium permanganate ($KMnO_4$, AR) were obtained from Chengdu Haihong Chemicals. Dimethylacetamide (DMAc, AR), *N*-methylpyrrolidone (NMP, AR), and potassium carbonate (K_2CO_3, AR) were provided by Tianjin BODI chemicals. Graphene was supplied by XFNANO Materials Tech Co. Ltd. All the materials were used without further purification.

Synthesis of SPEN and SGO

The SPEN was synthesized via nucleophilic aromatic substitution reaction from 2,6-difluorobenzonitrile (DFBN), 4,4′-biphenol (BP) and potassium 2,5-dihydroxybenzenesulfonate (SHQ) according to previous literature reported [34]. The schematic of diagrams to synthesize SPEN is shown in Scheme 1.

Graphene oxide (GO) was synthesized by the modified Hummers' method [35]: concentrated H_2SO_4 (240 ml) and H_3PO_4 (27 ml) were added into a 500 ml three-neck flask with a mixture of 2 g flaky graphite and 12 g $KMnO_4$. The reaction was heated to 50 °C with stirring for 12 h under sonicating. When the reaction finished, 30% H_2O_2 was poured into the mixture until the colour of the solution changed to golden. The product was washed with deionized water until the pH reaches 6–7.

The procedure for preparing SGO was as follows: 1 g GO was added in 30 ml H_2SO_4 with mechanical stirring for 3 h, then reacted at 100 °C for another 3 h. Furthermore, the product was washed with deionized water to neutral, vacuum filtrated, and dried in oven at 80 °C for 24 h (Scheme 2).

Preparation of SGO/SPEN composite membranes

The SGO/SPEN composite membranes were prepared by solution-casting method. The membranes were obtained by a homogeneous solution of SPEN and SGO under sonication in mixed solvent of DMAc and deionized water (*v*/v = 5:1). The mixture solution was spread on a horizontal and clean glass plate. The following temperature program is carried out to complete removal of solvent at 80,100,140, and 160 °C (each for 2 h), respectively. After cooling to room temperature naturally, the SGO/SPEN composite membranes with different SGO loading (0, 0.5, 1, and 2 wt%) were manufactured. The acid-form membranes were obtained by immersing the corresponding potassium form in H_2SO_4 for 24 h at room temperature.

Characterization

FTIR spectra were measured by using Shimadzu FTIR8400S Fourier Transform Infrared spectrometer under air atmosphere. The microstructures of membranes were tested with a high-resolution scanning electron microscope (SEM, JEOL JSM-5900LV) and all the samples of membranes were brittle fractured under liquid nitrogen atmosphere before measurement. Thermogravimetric analysis (TGA) was carried at by using a TA Instruments TGA-Q50 module. The sample of membranes for TGA analysis were preheated under nitrogen atmosphere from room temperature to 150 °C at a heating rate of 10 °C/min and held isothermally for 15 min for moisture removal, then heated from 80 to 600 °C at 20 °C/min. Powder samples were analysed by X-ray diffraction with the diffraction angle range of 5°–80° (RINT 2400 vertical goniometer (Rigaku, Japan)). The mechanical properties of the samples were recorded with a desktop electromechanical universal

Scheme 1 The schematic of diagrams to synthesize SPEN

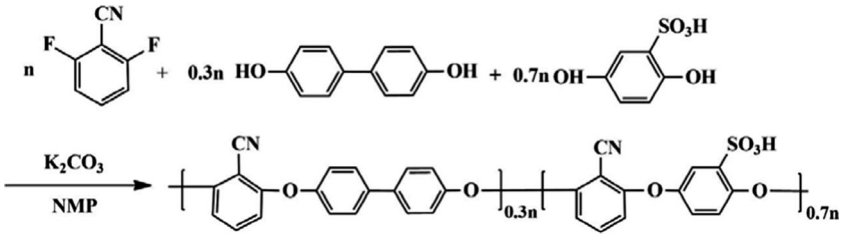

testing machine (SANS CMT6104 series) with an operating rate of 5 mm/min.

Water uptake and swelling ratio

The water uptake and swelling ratio were calculated by comparing the weight and dimension difference between dry and wet membranes. The membranes were dried in oven at 80 °C for 24 h prior to the measurements, and then the weights and lengths of dry membranes were measured. Finally, the membranes were immersed in deionized water for 24 h at predetermined temperatures. The water uptake rate and swelling ratio were calculated using the following equation:

$$\text{Water uptake}(\%) = \frac{W\text{wet} - W\text{dry}}{W\text{dry}} \times 100\% \quad (1)$$

$$\text{Swelling ratio}\ (\%) = \frac{L\text{wet} - L\text{dry}}{L\text{dry}} \times 100\% \quad (2)$$

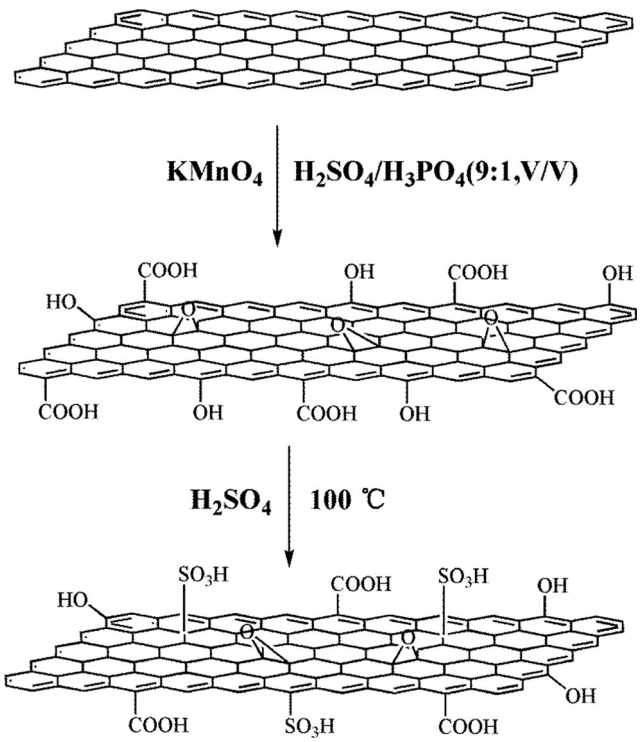

Scheme 2 The schematic diagram of the sulfonation process of GO

IEC

The ion-exchange capacity (IEC) of pure SPEN and composite membranes (GO/SPEN and SGO/SPEN) were measured via acid - base titration method. The dried acid form membranes were soaked in 50 ml NaCl solution (1 M) to completely displace H^+ into solution. 0.01 M NaOH solution with phenolphthalein as the pH indicator was used to titrate the concentration of H^+. Finally, IEC was calculated by the following equation:

$$\text{IEC} = \frac{V_{\text{NaOH}} \times C_{\text{NaOH}}}{W_{\text{dry}}} \quad (3)$$

where V_{NaOH} is the comsumed volume of NaOH, C_{NaOH} is the molar concentration of the titration, W_{dry} is the weight of the dried membranes.

Proton conductivity

The proton conductivity of the pure and blend membranes were measured by AC impedance spectroscopy (CHI650E, shanghai) over frequencies ranging from 0.1 to 100 kHz in potentiostatic mode with 50 mV. Before the conductivity experiment, all the membranes were immersed in deionized water for 24 h at predetermined temperatures. The proton conductivity was calculated by the following formula:

$$\sigma = \frac{L}{RA} \quad (4)$$

where σ is the proton conductivity of membranes, L is the thickness, A represents the cross-sectional area of the membrane, R is the resistance value.

Methanol permeability

The methanol permeability of the pure SPEN and blend membranes was carried out in two separate cells at room temperature, where one was filled with 10 M methanol solution (A, 16 ml) and another was filled with deionized water (B, 16 ml). The membranes were sandwiched between the two cells. The final concentration of methanol in reservoir is measured by using

SHIMADZU GC-8A chromatograph. The methanol permeability was calculated by the following formula:

$$C_B(t) = \frac{A}{V_B}\frac{DK}{L}C_A(t-t_0) \quad (5)$$

Where C_A, C_B are the methanol concentration of donor and receptor cells, A, L represent diffusion effective area and the thickness of membranes, V_B is the volume of reservoir B.

Results and discussion

Characterization of sulfonated graphene oxide

Structural characterization of GO and SGO

To prove the formation of SGO, the FTIR spectra of SGO and GO are recorded and shown in Fig. 1a**.** The GO shows characteristic absorption peaks at 1732 and 3424 cm^{-1}, which is ascribed to the stretching vibration of C = O from the carboxyl group and O–H bonds, respectively. For SGO, it is clearly observed that new absorption bands appear at 1088 and 1033 cm^{-1}, which belongs to the absorption of O = S = O asymmetric and symmetric stretching vibrations.

The TGA curves of SGO and GO are shown in Fig. 1b**.** The TGA curves of SGO and GO are shown in Fig. 1b. A loss weight can be observed at below 150 °C, which is the adsorbed and bounded water. GO which contains various oxygen functional groups can be easily decomposed at 150–200 °C. After sulfonation, the initial decomposition temperature of SGO is above 230 °C, which is the decomposition of sulfonic acid groups. The discrepancy is the result from the decomposition of different functional groups, suggesting the successful introduction of the sulfonic acid groups. Furthermore, XRD patterns of SGO and GO are presented in Fig. 2**.** The sharp diffraction peak of GO can be observed at 10.2°, which indicates the interlayer spacing of GO is about 0.86 nm. SGO has a diffraction angle at 25.2° and the layer-to-layer distance of SGO is about 0.35 nm. The reduction in interlayer spacing is caused by the partial restacking through π–π interaction and the removal of oxygen functional groups after sulfonation, which is consistent with the reported literature [36]. The shifting of the diffraction peak toward the higher 2θ is due to the introduction of sulfonic acid groups [29].

SEM characterization

The SEM images of SGO/SPEN and GO/SPEN composite membranes with different loading of GO and SGO at the 20,000 magnification times are shown in Fig. 3**.** Compared with GO/SPEN membranes, the SGO/SPEN membranes show less obvious crack and good interface compatibility, indicating the better interfacial interaction, which is the prerequisite for excellent performances of membranes. Furthermore, the composite membranes with low content particles such as 0.5 and 1 wt% show good interfacial compatibility between the filler and polymer. With the further increase of SGO fillers, the interface interaction between fillers and SPEN matrix is weaker than 1 wt% SGO/SPEN due to phase separation.

Thermal analysis

The TGA curves of pure SPEN and SGO/SPEN blend membranes are shown in Fig. 4. The initial thermal decomposition temperature of SGO/SPEN composite membranes is about 265 °C, while the initial decomposition temperature of pure membrane at 253 °C. The results demonstrate that the thermal stability of the membranes has improved by the SGO. The 5 and 10% weight loss temperatures are in the range of 356–358 °C and 370–372 °C, respectively, showing that the composite membranes possess good heat resistance.

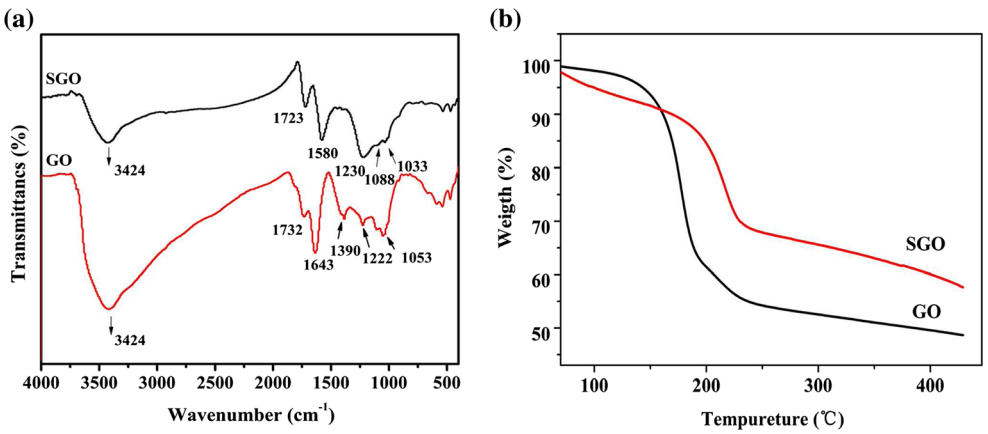

Fig. 1 **a** FTIR spectra of GO and SGO. **b** TGA curves of GO and SGO

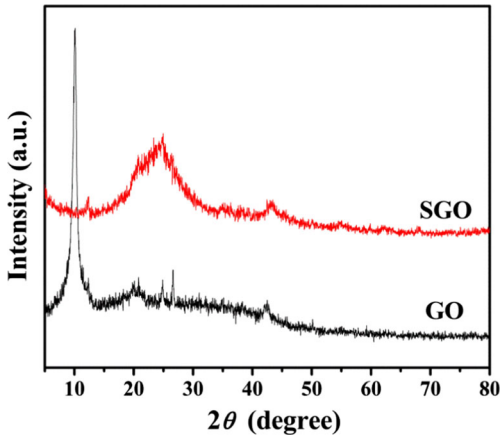

Fig. 2 XRD patterns of SGO and GO

Water uptake and swelling ratio

The water uptake and swelling ratio have a certain effect on the proton conductivity and dimensional stability of the membranes. The adsorbed water is propitious to the protons transport and the sulfonic acid group also plays an important role in the process of water uptake [37–39]. Furthermore, the intermolecular interactions and microstructure of the membranes also affect the water uptake and swelling ratio. The water uptake and swelling ratio of pure membrane and GO/SPEN or SGO/SPEN composite films with varied temperatures are shown in Fig. 5 and Table 1. In general, with the temperature increasing, the water uptake and swelling rate of the membrane also increase. Due to excessive swelling or even dissolution of the pure membrane at 80 °C, the water uptake of pure membrane cannot be measured. Comparing with pure membranes, the water uptake and swelling ratio of blend membranes are lower than that of the former. This is attributed to the enhancement of the interfacial interaction between filler and polymer (such as hydrogen bonds). The water uptake of SGO is lower than that of GO due to the better interfacial adhesion, which is corresponding to the result of SEM images. Hence, the SGO/SPEN composite membranes have a more closely membrane structure, leading to the lower water uptake and swelling ratio.

IEC

The values of IEC are related to the content of sulfonic acid groups. The IEC values of pure and composite membranes (at room temperature) are presented in Table 2. The IEC values of SGO/SPEN composite membranes are increased with the increase of the sulfonic acid group. Meanwhile, the IEC of

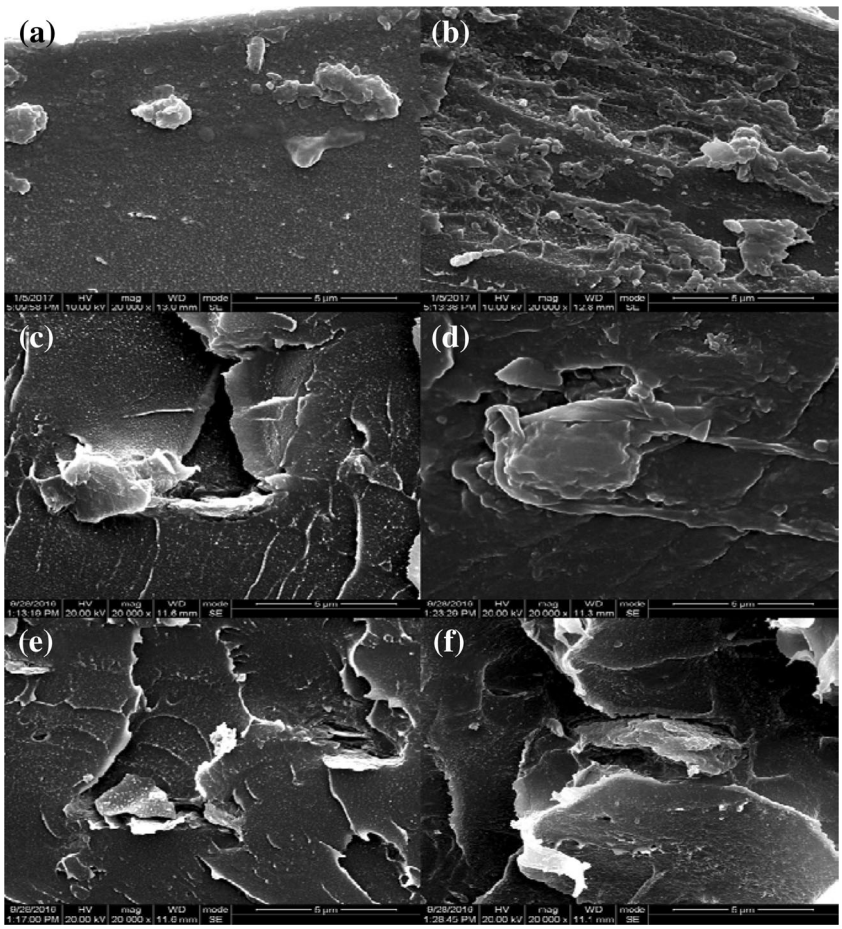

Fig. 3 The SEM images of SPEN composite membranes with (**a**) 0.5 wt% GO loadings, (**b**) 0.5 wt% SGO loadings, (**c**) 1 wt% GO loadings, (**d**) 1 wt% SGO loadings, (**e**) 2 wt% GO loadings, and (**f**) 2 wt% SGO loadings at the 20,000 magnification time

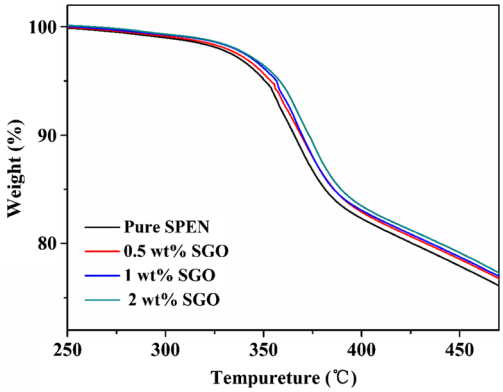

Fig. 4 The TGA curves of pure and SGO/SPEN composite membranes

SGO/SPEN membranes are higher than that of pure membrane and GO/SPEN composite membranes. The result is ascribed to the fact that SGO provides more sulfonic acid groups as fixed charge sites and effects the IEC of SGO/SPEN composite membranes. In addition, the values of GO/SPEN blend films are decreased with the addition of GO, which is due to the non-proton-conducting characteristic of GO.

Mechanical properties

Fig. 6 shows the tensile strength, modulus and elongation at break of pure SPEN and composite membranes (SGO/SPEN and GO/SPEN) measured at room temperature in the dry state. The mechanical strength and modulus of SGO/SPEN composite membranes with the 1 wt% content reach the maximum value of 52.1 and 1876.2 MPa, respectively, and then decrease with further addition of SGO or GO filler. Compared with GO/SPEN membranes, SGO/SPEN membranes possess better mechanical properties. This result is attributed to the increased interfacial interaction between fillers and polymer, which is coincident with the results of SEM images. With the further increases of particle content, the tensile strength and modulus of composite membranes are mainly affected by the phase separation with SPEN. When the particle content is over than 1 wt%, the dispersion and compatibility of SGO and SPEN becomes worse. Besides, it is obvious that the elongation at break of SPEN composite membranes (SGO/SPEN and GO/SPEN) decreases with increasing the content of particles. This is attributed to strong interaction between

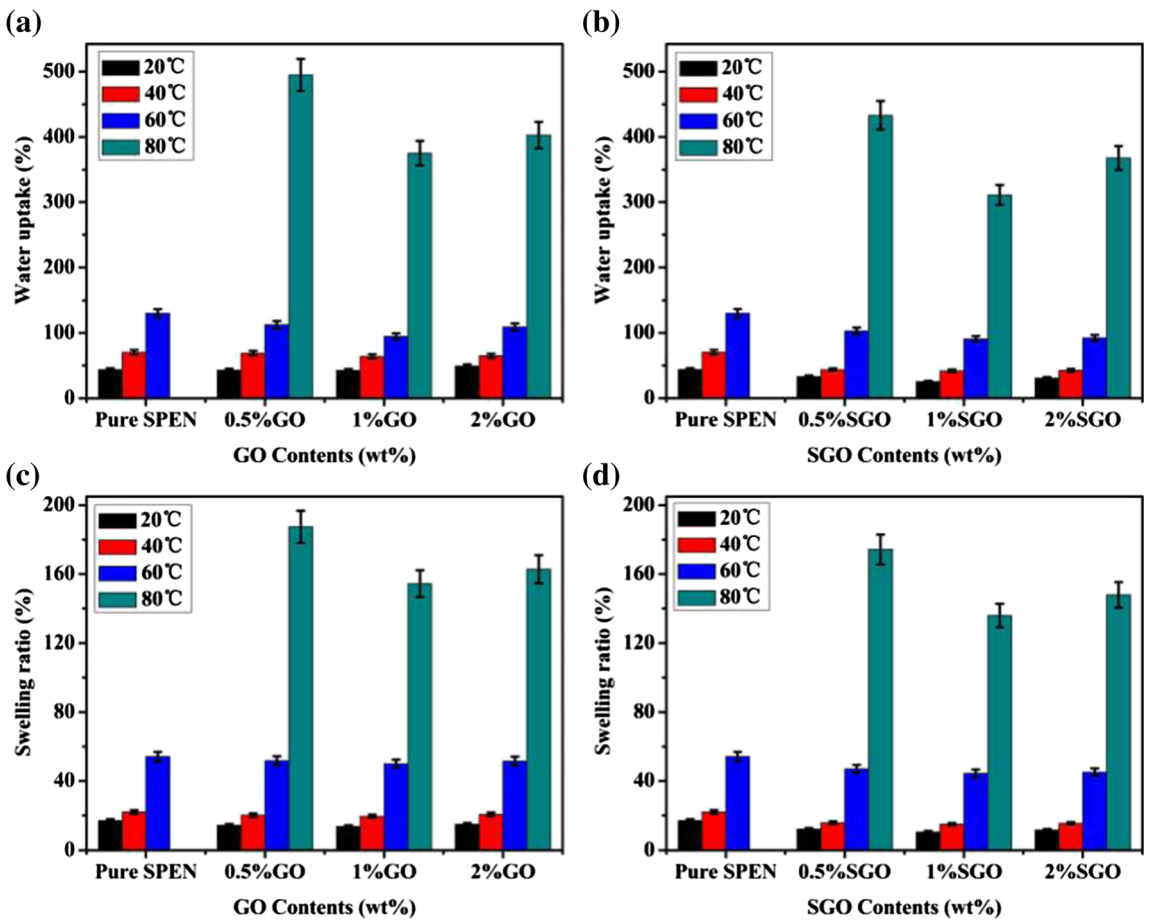

Fig. 5 The water uptake and swelling ratio of pure and GO/SPEN composite membranes (**a**, **c**) and SGO/SPEN composite membranes (**b**, **d**) with the variation of temperatures

Table 1 The water uptake and swelling ration of pure membrane and GO/SPEN or SGO/SPEN composite films with the change in temperature

Filler contents	Water uptake (%)				Swelling ratio (%)			
	20 °C	40 °C	60 °C	80 °C	20 °C	40 °C	60 °C	80 °C
Pure SPEN	43.75	70.22	129.78	/	17	22	54.25	/
0.5% GO	43.02	68.91	112.52	494.61	14.31	20.18	51.87	187.42
1% GO	42.6	63.98	94.58	375.3	13.57	19.45	49.98	154.38
2% GO	49.37	64.91	109.71	402.82	14.92	20.65	51.62	162.75
0.5% SGO	33.05	43.5	90.47	433	12.09	15.77	46.96	174.23
1% SGO	25.25	41.73	92.47	311.15	10.55	14.84	44.35	135.92
2% SGO	30.76	42.39	92.05	367.86	11.57	15.36	45.02	147.87

fillers and the SPEN and enhanced inflexibility of the SPEN chains caused by existence of GO and SGO, which hinder the movement of the polymer chains [42, 43]. In all, all the membranes possess good mechanical properties, which is enough for the applications as proton exchange membrane.

Proton conductivity

In the direct methanol fuel cell application, the most basic parameters are the proton conductivity and methanol permeability. The proton conductivities of pure membrane and composite membranes (GO/SPEN and SGO/SPEN) are shown in Fig. 7 and Table 2**.** The proton conductivity of GO/SPEN composite membranes are higher than that of pure SPEN, which is owing to the formation of hydrogen bond between hydroxyl or carboxylic and sulfonic acid groups, and benefit to the proton transfer via proton hoping based on the Grotthus mechanism [33, 44]. Besides, the proton conductivity of SGO/SPEN membranes has increasing trend with the addition of SGO. As the loading of SGO above 1 wt%, the proton conductivity reaches the highest value, while the SGO content is further increased, the proton conductivity of SGO/SPEN membrane decreases. The primary reason of above phenomenon is that SGO can provide excessive sulfonic acid groups, which plays an important role in the enhancement of proton conductivity. However, when beyond a certain range, the interfacial adhesion between the SGO and SPEN becomes worse, which can damage the proton transfer and influence the proton transfer efficiency.

The proton conductivity of composite membranes with variation of temperatures is shown in Fig. 7**.** Normally, the proton conductivity of the blend membranes increases with the increasing temperature, which is caused by the accelerated movement of water molecules to benefit the proton hoping or diffusing in the membranes [45]. In short, the SGO/SPEN membranes with 1 wt% SGO show excellent proton conductivity, which is higher than that of Nafion 117 and other reported SGO hybrid membrane [40, 41].

Methanol permeability and selectivity

In DMFC application, the ideal PEM should possess high conductivity and low methanol permeability simultaneously. The methanol permeability and selectivity of pure SPEN and composite membranes are presented in Table 2**.** From the results, it is clear that the methanol permeability of composite

Table 2 The IEC, proton conductivity, methanol permeation, selectivity of pure and composite membranes at 20 °C

The contents of fillers	IEC (mmol/g)	Proton conductivity (S/cm)	Methanol permeation (10^{-6} cm^{-2}/s)	Selectivity (10^5 S cm^{-3} s)
Pure SPEN	1.672	0.09	0.67	1.343
0.5 wt% GO	1.636	0.093	0.42	2.214
1 wt% GO	1.588	0.099	0.21	4.714
2 wt% GO	1.503	0.092	0.36	2.556
0.5 wt% SGO	1.761	0.099	0.38	2.605
1 wt% SGO	1.839	0.109	0.17	6.412
2 wt% SGO	1.878	0.098	0.28	3.5
5 wt% SGO/SPEEK [40]	1.65	0.084	0.38	2.211
0.5 wt% SGO/Nafion [41]	-	0.0367	0.0916	4.01
Nafion 117	-	0.064	1.41	0.45

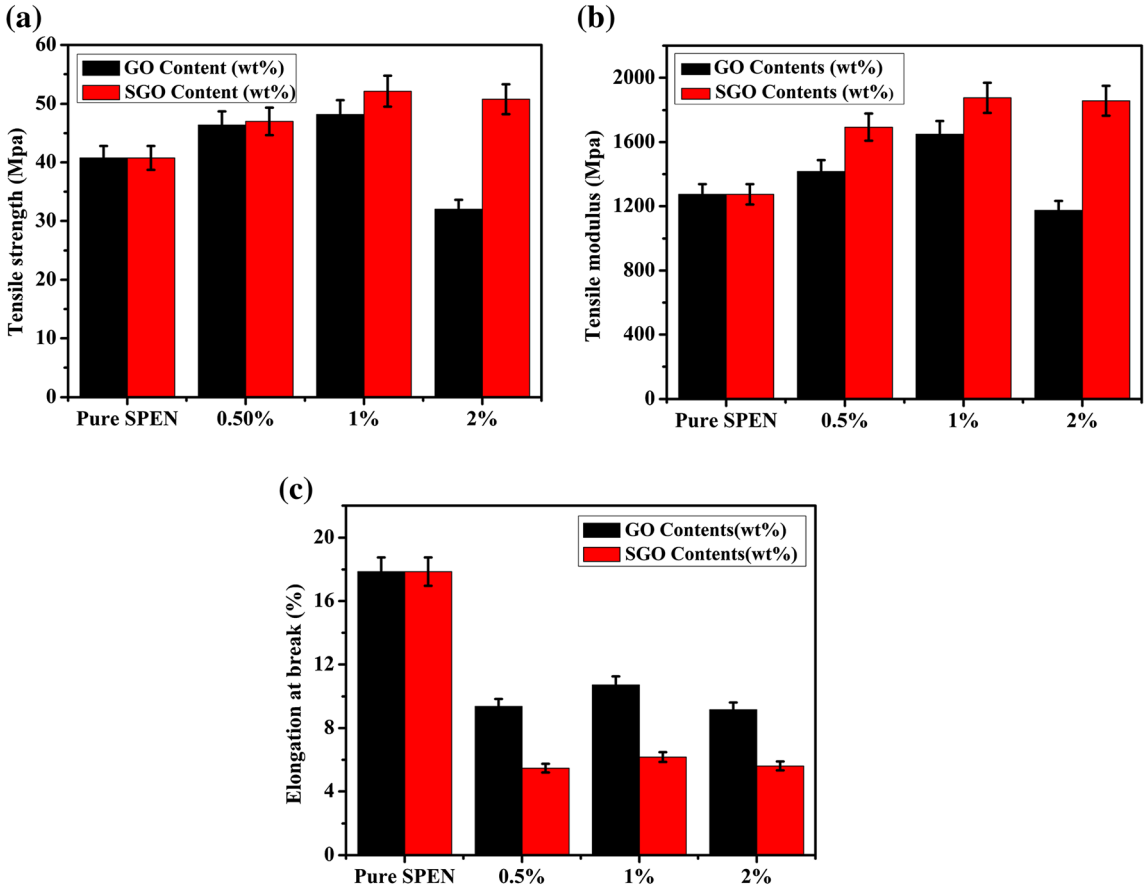

Fig. 6 The (**a**) tensile strength, (**b**) modulus and (**c**) elongation at break of pure SPEN and composite membranes (SGO/SPEN and GO/SPEN) measured at room temperature in the dry state

membranes decreases with the increase of GO or SGO particle content. GO and SGO hinder the methanol permeation through the hybrid membrane and act as barriers for the connected hydrophilic. Besides, the better interfacial interaction between SGO and SPEN also can decrease the methanol crossover of membranes. As noted above, the interfacial adhesion of SGO/SPEN membrane is stronger than GO/SPEN membrane. The SGO/SPEN membranes hinder the migration of methanol molecules more effectively than the GO/SPEN membrane.

Generally, the selectivity (defined as the ratio of the proton conductivity to the methanol permeability of the membrane) is often used to estimate the DMFC performance and membranes with a higher selectivity exhibit better DMFC performance [46, 47]. In Table 2, the SGO/SPEN with 1% SGO loading has a higher selectivity (6.412×10^5 S s cm^{-3}), which

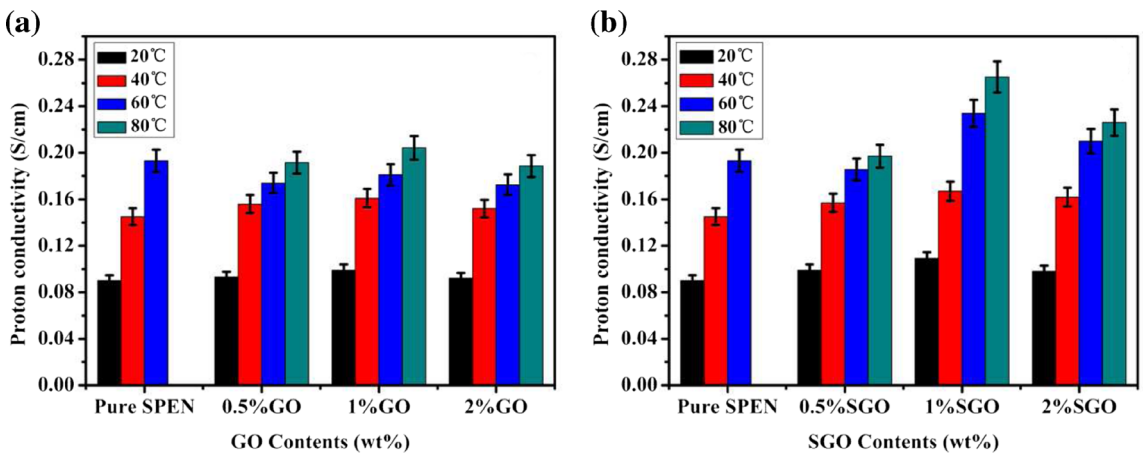

Fig. 7 The proton conductivity of pure and (**a**) GO/SPEN composite and (**b**) SGO/SPEN composite membranes with variation of temperatures

is higher than that of Nafion 117 and other SGO hybrid membranes [40, 41]. All these results prove the composite membranes to be potential proton exchange membranes for fuel cell applications.

Conclusions

In summary, the SGO was prepared by direct sulfonate method and the SGO/SPEN composite membranes were fabricated by solution-casting. The FTIR, TGA and XRD confirmed the successful formation of SGO. The microstructure and compatibility between filler and SPEN matrix were observed by SEM. The membrane with 1 wt% SGO possesses excellent interfacial compatibility, which is the prerequisite for the better dimensional stability, high proton conductivity and low methanol permeation., The proton conductivity of composite membrane with 1 wt% SGO loading reached 0.109 S/cm at 20 °C, increased by 70.13% compared with Nafion 117, showing excellent proton transfer capability. Meanwhile, the methanol permeability decreased by 87.9% than that of the commercial Nafion117 membrane. Based on these results, direct sulfonate to obtain SGO is a facile, effective and low cost method to enhance the comprehensive performances of SPEN as the application of proton exchange membrane and SGO/SPEN composite membranes can be considered to be promising candidate for application in fuel cells.

Acknowledgements The authors wish to thank for financial support of this work from the National Natural Science Foundation (Nos. 51373028) and University of Electronic Science and Technology of China (A03013023601011).

References

1. Shrivastava NK, Thombre SB, Chadge RB (2016) Liquid feed passive direct methanol fuel cell: challenges and recent advances. Ionics 22:1–23
2. Falcão DS, Oliveira VB, Rangel CM, Pinto AMFR (2014) Review on micro-direct methanol fuel cells. Renew Sust Energ Rev 34:58–70
3. Munjewar SS, Thombre SB, Mallick RK (2017a) A comprehensive review on recent material development of passive direct methanol fuel cell. Ionics 23:1–18
4. Faghri A, Guo Z (2008) An innovative passive DMFC technology. Appl Therm Eng 28:1614–1622
5. Munjewar SS, Thombre SB, Mallick RK (2017b) Approaches to overcome the barrier issues of passive direct methanol fuel cell-review. Renew Sust Energ Rev 67:1087–1104
6. Hashemi R, Yousefi S, Faraji M (2015) Experimental studying of the effect of active area on the performance of passive direct methanol fuel cell. Ionics 21:2851–2862
7. Yousefi S, Zohoor M (2014) Conceptual design and statistical overview on the design of a passive DMFC single cell. Int J Hydrog Energy 39:5972–5980
8. Ting G, Sun J, Deng H, Jiao K, Huang XR (2015) Transient analysis of passive direct methanol fuel cells with different operation and design parameters. Int J Hydrog Energy 40:14978–14995
9. Yousefi S, Shakeri M, Sedighi K (2013) The effect of cell orientations and environmental conditions on the performance of a passive DMFC single cell. Ionics 19:1637–1647
10. Yousefi S, Ganji DD (2012) Experimental investigation of a passive direct methanol fuel cell with 100 cm^2 active areas. Electrochim Acta 85:693–699
11. Ting G, Sun J, Deng H, Xie X, Jiao K, Huang X (2016) Investigation of cell orientation effect on transient operation of passive direct methanol fuel cells. Int J Hydrog Energy 41:6493–6507
12. Wang Y, Chen KS, Mishler J, Cho SC, Adroher XC (2011) A review of polymer electrolyte membrane fuel cells: technology, applications, and needs on fundamental research. Appl Energy 88:981–1007
13. Papadimitriou KD, Paloukis F, Neophytides SG, Kallitsis JK (2011) Cross-linking of side chain unsaturated aromatic polyethers for high temperature polymer electrolyte membrane fuel cell applications. Macromolecules 44:4942–4951
14. Devrim Y, Erkan S, Bac N, Eroglu I (2012) Improvement of PEMFC performance with Nafion/inorganic nanocomposite membrane electrode assembly prepared by ultrasonic coating technique. Int J Hydrog Energy 37:16748–16758
15. Song MF, Lu XW, Li ZF, Liu GH, Yin XY, Wang YX (2016) Compatible ionic crosslinking composite membranes based on SPEEK and PBI for high temperature proton exchange membranes. Int J Hydrog Energy 41:12069–12081
16. Sacca A, Carbone A, Gatto I, Pedicini R, Freni A, Patti A, Passalacqua E (2016) Composites Nafion-titania membranes for polymer electrolyte fuel cell (PEFC) applications at low relative humidity levels: chemical physical properties and electrochemical performance. Polym Test 56:10–18
17. Li JC, Zhang YP, Zhang S, Huang XD (2015) Sulfonated polyimide/s-MoS2 composite membrane with high proton selectivity and good stability for vanadium redox flow battery. J Membr Sci 490:179–189
18. Chen L, Pu ZJ, Long Y, Tang HL, Liu XB (2014) Synthesis and properties of sulfonated poly(arylene ether nitrile) copolymers containing carboxyl groups for proton-exchange membrane materials. J Appl Polym Sci 131:40213
19. Gahlot S, Kulshrestha V (2015) Dramatic improvement in water retention and proton conductivity in electrically aligned functionalized CNT/SPEEK Nanohybrid PEM. ACS Appl Mater Interfaces 7:264–272
20. Li HQ, Liu XJ, Xu JM, Xu D, Ni HZ, Wang S, Wang Z (2016) Enhanced proton conductivity of sulfonated poly(arylene ether ketone sulfone) for fuel cells by grafting triazole groups onto polymer chains. J Membr Sci 509:173–181
21. Lee C-H, Wang Y-Z (2008) Synthesis and characterization of epoxy-based semi-interpenetrating polymer networks sulfonated polyimides proton-exchange membranes for direct methanol fuel cell applications. J Polym Sci, Part A: Polym Chem 46:2262–2276
22. Feng M, You Y, Zheng P, Liu J, Jia K, Huang Y, Liu X (2016) Low-swelling proton-conducting multi-layercomposite membranes containing polyaryleneether nitrile and sulfonated carbon nanotubes for fuel cells. Int J Hydrog Energy 41:5113–5122
23. Laberty-Robert C, Vallé K, Pereira F, Sanchez C (2011) Design and properties of functional hybrid organic–inorganic membranes for fuel cells. Chem Soc Rev 40:961–1005
24. Kango S, Kalia S, Celli A, Njuguna J, Habibi Y, Kumar R (2013) Surface modification of inorganic nanoparticles for development of organic–inorganic nanocomposites–a review. Prog Polym Sci 38:1232–1261

25. Yu HL, Wang TS, Wen B, Lu MM, Xu Z, Zhu CL, Chen YJ, Xue XY, Sun CW, Cao MS (2012) Graphene/polyaniline nanorod arrays: synthesis and excellent electromagnetic absorption properties. J Mater Chem 22:21679–21685
26. Zhan YQ, Yang XL, Guo H, Yang J, Meng FB, Liu XB (2012a) Cross-linkable nitrile functionalized graphene oxide/poly(arylene ether nitrile) nanocomposite films with high mechanical strength and thermal stability. J Mater Chem 22:5602–5608
27. Zhan YQ, Yang J, Zhou YK, Yang XL, Meng FB, Liu XB (2012b) Nitrile functionalized graphene for poly(arylene ether nitrile) nanocomposite films with enhanced dielectric permittivity. Mater Lett 78:88–91
28. Huang Y, Qi Q, Pan H, Lei X, Liu X (2016) Facile preparation of octahedral Fe_3O_4/RGO composites and its microwave electromagnetic properties. J Mater Sci Mater Electron 27:9577–9583
29. Gahlot S, Sharma PP, Kulshrestha V, Jha PK (2014) SGO/SPES-based highly conducting polymer electrolyte membranes for fuel cell application. ACS Appl Mater Interfaces 6:5595–5601
30. Jiang ZQ, Zhao XS, Manthiram A (2013) Sulfonated poly(ether ether ketone) membranes with sulfonated graphene oxide fillers for direct methanol fuel cells. Int J Hydrog Energy 38:5875–5884
31. Beydaghi H, Javanbakht M, Kowsari E (2014) Synthesis and characterization of poly(vinyl alcohol)/SulfonatedGraphene oxide nanocomposite membranes for use in proton exchange membrane fuel cells (PEMFCs). Ind Eng Chem Res 53:16621–16632
32. Xu CX, Cao YC, Kumar R, Wu X, Wang X, Scott K (2011) A polybenzimidazole/sulfonated graphite oxide composite membrane for high temperature polymer electrolyte membrane fuel cells. J Mater Chem 21:11359–11364
33. Kumar R, Mamlouk M, Scott K (2014) Sulfonated polyether ether ketone-sulfonated graphene oxide composite membranes for polymer electrolyte fuel cell. RSC Adv 4:617–623
34. Pu ZJ, Chen L, Long Y, Tong LF, Huang X, Liu XB (2013) Influence of composition on the proton conductivity and mechanicalproperties ofsulfonatedpoly(arylethernitrile) copolymers for proton exchange membranes. J Polym Res 20:281
35. Marcano DC, Kosynkin DV, Berlin JM, Sinitskii A, Sun ZZ, Slesarev A, Alemany LB, Lu W, Tour JM (2010) Improved synthesis of graphene oxide. ACS Nano 4:4806–4814
36. Liu J, Xue Y, Dai L (2012) Sulfated graphene oxide as a hole extraction layer in high- performance polymer solar cells. J Phys Chem Lett 3:1928–1933
37. Mohtar SS, Ismail AF, Matsuura T (2011) Preparation and characterization of SPEEK/MMT-STA composite membrane for DMFC application. J Membr Sci 371:10–19
38. Hasani-Sadrabadi MM, Dashtimoghadam E, Majedi FS, Moaddel H, Bertscha A, Renaud P (2013) Superacid-doped polybenzimidazole-decorated carbon nanotubes: a novel high-performance proton exchange nanocomposite membrane. Nano 5: 11710–11717
39. Buchmuller Y, Wokaun A, Gubler L (2014) Polymer-bound anti-oxidants in grafted membranes for fuel cells. J Mater Chem A 2: 5870–5882
40. HeoY IH, Kim J (2013) The effect of sulfonated graphene oxide on sulfonated poly (ether ether ketone) membrane for direct methanol fuel cells. J Membr Sci 425–426:11–22
41. Chien H-C, Tsai L-D, Huang C-P, Kang C-Y, Lin J-N, Chang F-C (2013) Sulfonated graphene oxide/Nafion composite membranes for high-performance direct methanol fuel cells. Int J Hydrog Energy 38:13792–13801
42. Raheela M, Yao K, Gong J, Chen XC, Liu DT, Lin YC, Cui DM, Siddiq M, Tang T (2015) Poly(vinyl alcohol)/GO-MMT nanocomposites: preparation. Structure and Properties Chin J Polym Sci 33: 329–338
43. Zhao X, Zhang QH, Chen DJ (2010) Enhanced mechanical properties of graphene-based poly(vinyl alcohol) composites. Macromolecules 43:2357–2363
44. Li L, Zhang J, Wang YX (2003) Sulfonated poly(ether ether ketone) membranes for direct methanol fuel cell. J Membr Sci 226:159–167
45. Bose S, KuilaT NTXH, Kim NH (2011) Polymer membranes for high temperature proton exchange membrane fuel cell: recent advances and challenges. Prog Polym Sci 36:813–843
46. Shin DW, Lee SY, Kang NR, Lee KH, Guiver MD, Lee YM (2013) Durable sulfonated poly(arylene sulfide sulfone nitrile)s containing naphthalene units for direct methanol fuel cells (DMFCs). Macromolecules 46:3452–3460
47. Chen Z, Holmberg B, Li W, Wang X, Deng W, Munoz R, Yan Y (2006) Nafion/zeolite nanocomposite membrane by in situ crystallization for a direct methanol fuel cell. Chem Mater 18:5669–5675